

# On Total Reuse of Krylov Subspaces for an iterative FETI-solver in multirate integration

Andreas S. Seibold\*, Daniel J. Rixen\*, Javier del Fresno Zarza\*

\* Chair of Applied Mechanics  
Technical University of Munich  
Munich, Germany

e-mail: {andreas.seibold, rixen, javier.fresno}@tum.de

**Key words:** FETI, Structural dynamics, Krylov-Subspaces, Recycling, Multirate Time-Integration

**Abstract:** *In this work, we adapt a Total Reuse of Krylov Subspaces for usage in a GMRES-solver and apply it to nonlinear structural-dynamics examples. These examples are then solved by a multirate FETI-method, the nonlinear BGC-macro method, which allows local subcycling in time within substructures, such that local time-stepping is performed between synchronization-time-steps. In these proposed examples, we show that the reuse-method reduces the total number of GMRES-iterations and shifts the eigenvalue-spectrum of the global system towards smaller eigenvalues.*

## 1 INTRODUCTION

Substructuring methods are widely valued for parallelizing large structural mechanics problems and a popular non-overlapping dual domain decomposition method is the *Finite Elements Tearing and Interconnecting* (FETI) method [4]. In cases of local computationally expensive dynamics in a substructure, e.g. due to local damage or contact, it might be favorable to adjust the time-step-sizes locally. For such an asynchronous or multirate time-integration, domain-decomposition-based methods have been developed, such as the linear subcycling-based GC-method by Gravouil and Combescure [10]. However, this method suffers from energy-dissipation and therefore the non-dissipative linear and nonlinear PH-methods by Prakash and Hjelmstad [15] and the linear BGC-macro [3] have been developed. Recently a nonlinear version of the BGC-macro method has been proposed [18] and applied to an iterative FETI-solver equipped with a Dirichlet-like preconditioner [19]. Hence, the next natural step is to further improve solver-efficiency by applying recycling-techniques to this new problem. In this work, we adapt a *Total Reuse of Krylov Subspaces* (TRKS) approach [9], successfully applied to linear and nonlinear structural dynamics in [12, 17], to a GMRES-solver and investigate its applicability to the nonlinear BGC-macro method.

In Section 2.1, we introduce the applied multirate-method nonlinear BGC-macro and, in Section 2.2, the TRKS and its application in a GMRES is described. Finally, we show in Section 3 numerical examples with the described methods and conclusions in Section 4.

## 2 FETI for nonlinear structural dynamics

For the parallelization of a Finite Elements discretized structural dynamics problem, we divide the structure spacially along the element's edges in non-overlapping substructures  $\Omega^{(s)}$ . These substructures are connected with Lagrange-multipliers  $\vec{\lambda}$ , that can be viewed as interface-forces, as stated in the FETI method [4]. In Section 2.1, we give a brief introduction to the governing equations and the multirate BGC-macro method and in Section 2.2, we describe the application of a TRKS method to a GMRES solver.

## 2.1 Multirate with nonlinear BGC-macro method

Throughout this work, we consider different time-step-sizes in each substructure, which is referred to as multirate or asynchronous time-integration. As depicted in Figure 1 for two substructures  $A$  and  $B$ , the global time-integration with time-steps  $n$  is sub-cycled with  $N_j$  smaller time-steps with size  $\Delta t^{(B)} = \frac{\Delta t^{(A)}}{N_j}$  on a micro-substructure.

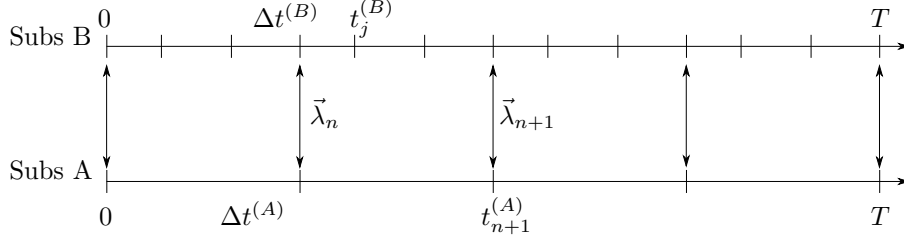


Figure 1: Multirate time-discretization.

The global time-steps are also referred to as macro-time-steps and the Lagrange-multipliers are interpolated linearly onto the local micro-timesteps

$$\vec{\lambda}_j = \left(1 - \frac{j}{N_j}\right) \vec{\lambda}_{n-1} + \frac{j}{N_j} \vec{\lambda}_n \quad (1)$$

resulting in the local differential equations of motion, written as a force-residual  $fr\vec{e}s_j^{(s)}$  here

$$fr\vec{e}s_j^{(s)} = \mathbf{M}^{(s)} \ddot{\vec{q}}_j^{(s)} + \vec{f}_{int}(\vec{q}_j^{(s)}) + \mathbf{B}^{(s)T} \vec{\lambda}_j - \vec{f}_{ext}(t_j) = \vec{0} \quad (2)$$

at a discrete time-step  $j$  with a mass-matrix  $\mathbf{M}^{(s)}$ , nonlinear internal forces  $\vec{f}_{int}$  and external forces  $\vec{f}_{ext}$ , as well as displacements  $\vec{q}^{(s)}$ , velocities  $\dot{\vec{q}}^{(s)}$  and accelerations  $\ddot{\vec{q}}^{(s)}$ . The Lagrange-multipliers  $\vec{\lambda}$  are applied to the local *degrees of freedom* (dof) by a signed Boolean matrix  $\mathbf{B}^{(s)}$ . The local solutions are then synchronized at the macro-time-scale, which is formulated by requiring the interface-velocities to coincide at the macro-timestep  $n$  in the interface-residual  $ir\vec{e}s_n$

$$ir\vec{e}s_n = \sum_{s=1}^{N_s} \mathbf{B}^{(s)} \dot{\vec{q}}_n^{(s)} = \vec{0}. \quad (3)$$

This approach is known from the linear BGC-macro method [3], which has been recently extended to nonlinear models [18]. To solve both equations (2) and (3), we choose as time-integration scheme one of the most popular ones, namely the Newmark- $\beta$  scheme [14]

$$\begin{aligned} ar\vec{e}s_j^{(s)} &= -\frac{1}{\gamma \Delta t} \dot{\vec{q}}_{j-1}^{(s)} - \frac{1-\gamma}{\gamma} \ddot{\vec{q}}_{j-1}^{(s)} + \frac{1}{\gamma \Delta t} \dot{\vec{q}}_j^{(s)} - \ddot{\vec{q}}_j^{(s)} = \vec{0} \\ ar\vec{e}s_j^{(s)} &= \dot{\vec{q}}_{j-1}^{(s)} + \left(1 - \frac{\beta}{\gamma}\right) \Delta t \dot{\vec{q}}_{j-1}^{(s)} + \left(\frac{1}{2} - \frac{\beta}{\gamma}\right) \Delta t^2 \ddot{\vec{q}}_{j-1}^{(s)} + \frac{\beta}{\gamma} \Delta t \dot{\vec{q}}_j^{(s)} - \dot{\vec{q}}_j^{(s)} = \vec{0}, \end{aligned}$$

with  $\beta \in [0, 1/4]$ ,  $\gamma \in [0, 1/2]$ . The equations have been reformulated in residual-form  $ar\vec{e}s_j^{(s)}$  and  $ir\vec{e}s_j^{(s)}$  here. Analogously to the classical single-rate FETI in Farhat e.a. [6] and the

PH-method [15], all these equations are linearized for  $\ddot{q}_j^{(s)}$ ,  $\dot{q}_j^{(s)}$ ,  $\bar{q}_j^{(s)}$  and  $\vec{\lambda}_n$ , resulting in

$$\tilde{\mathbf{M}}^{(s)} = \begin{bmatrix} \mathbf{M}^{(s)} & \mathbf{0} & \mathbf{K}^{(s)} \\ -\gamma\Delta t^{(s)}\mathbf{I} & \mathbf{I} & \mathbf{0} \\ -\beta\Delta t^{(s)2}\mathbf{I} & \mathbf{0} & \mathbf{I} \end{bmatrix} \quad \tilde{\mathbf{C}}^{(s)} = \begin{bmatrix} \mathbf{B}^{(s)T} \\ \mathbf{0} \\ \mathbf{0} \end{bmatrix} \quad \tilde{\mathbf{r}}_j^{(s)} = \begin{bmatrix} fr\vec{e}s_j^{(s)} \\ ar\vec{e}s_j^{(s)} \\ dr\vec{e}s_j^{(s)} \end{bmatrix}$$

$$\mathbf{N}^{(s)} = \begin{bmatrix} \mathbf{0} & \mathbf{0} & \mathbf{0} \\ -\Delta t^{(s)}(1-\gamma)\mathbf{I} & -\mathbf{I} & \mathbf{0} \\ -\Delta t^{(s)}(1/2-\beta)\mathbf{I} & -\Delta t^{(s)}\mathbf{I} & -\mathbf{I} \end{bmatrix} \quad \tilde{\mathbf{B}}^{(s)T} = \begin{bmatrix} \mathbf{0} \\ \mathbf{B}^{(s)T} \\ \mathbf{0} \end{bmatrix} \quad \tilde{\mathbf{q}}_j^{(s)} = \begin{bmatrix} \ddot{q}_j^{(s)} \\ \dot{q}_j^{(s)} \\ \bar{q}_j^{(s)} \end{bmatrix}$$

$$\underbrace{\begin{bmatrix} \tilde{\mathbf{M}}_1^{(s)} & & & & \\ \mathbf{N}^{(s)} & \tilde{\mathbf{M}}_2^{(s)} & & & \\ & \ddots & \ddots & & \\ & & \mathbf{N}^{(s)} & \tilde{\mathbf{M}}_{N_j}^{(s)} & \\ & & & & \end{bmatrix}}_{\mathbf{A}^{(s)}} \underbrace{\begin{bmatrix} \Delta\tilde{q}_1^{(s)} \\ \Delta\tilde{q}_2^{(s)} \\ \vdots \\ \Delta\tilde{q}_{N_j}^{(s)} \end{bmatrix}}_{\Delta\tilde{\mathbf{q}}^{(s)}} + \underbrace{\begin{bmatrix} \frac{1}{N_j}\tilde{\mathbf{C}}^{(s)} \\ \frac{2}{N_j}\tilde{\mathbf{C}}^{(s)} \\ \vdots \\ \frac{N_j}{N_j}\tilde{\mathbf{C}}^{(s)} \end{bmatrix}}_{\tilde{\mathbf{C}}^{(s)}} \Delta\vec{\lambda}_n = \underbrace{\begin{bmatrix} -\tilde{r}_1^{(s)}(\tilde{q}_0^{(s)}, \tilde{q}_1^{(s)}, \vec{\lambda}_1) \\ -\tilde{r}_2^{(s)}(\tilde{q}_1^{(s)}, \tilde{q}_2^{(s)}, \vec{\lambda}_2) \\ \vdots \\ -\tilde{r}_{N_j}^{(s)}(\tilde{q}_{N_j-1}^{(s)}, \tilde{q}_{N_j}^{(s)}, \vec{\lambda}_n) \end{bmatrix}}_{\tilde{\mathbf{r}}^{(s)}}$$

This local problem is solved for the local states  $\tilde{q}_j^{(s)}$  and inserted into the compatibility condition

$$\bar{\mathbf{B}}^{(s)}\Delta\tilde{\mathbf{q}}^{(s)} = \begin{bmatrix} \mathbf{0} & \dots & \mathbf{0} & \tilde{\mathbf{B}}^{(s)} \end{bmatrix} \Delta\tilde{\mathbf{q}}^{(s)} = -Ir\vec{e}s_n(\tilde{q}_{N_j}^{(s)})$$

$$\vec{r}_k = \underbrace{\sum_{s=1}^{N_s} \bar{\mathbf{B}}^{(s)} \mathbf{A}^{(s)-1} \tilde{\mathbf{C}}^{(s)}}_{\mathbf{F}} \Delta\vec{\lambda}_n - \underbrace{\left( \sum_{s=1}^{N_s} \bar{\mathbf{B}}^{(s)} \mathbf{A}^{(s)-1} \tilde{\mathbf{r}}^{(s)} + Ir\vec{e}s_n(\tilde{q}_{N_j}^{(s)}) \right)}_{\vec{d}} = \vec{0},$$

where  $\mathbf{A}^{(s)}$  is invertible due to the regularizing nature of the mass-matrix. This is the so-called interface-problem and its only unknown are the global interface-forces. In contrast to the classical FETI-method, the interface-operator  $\mathbf{F}$  is non-symmetric, which implies that we have to use a *Generalized Minimal Residual* (GMRES) method [16] here, as a Conjugate Gradient requires the problem to be symmetric.

## 2.2 TRKS for GMRES

The general idea of recycling relies on constructing an auxiliary coarse-space  $\mathbf{C}$  similarly to the natural or kernel coarse space in FETI for statical problems. Hence, this is usually referred to as two-level FETI [7]. This auxiliary coarse-space can be built on FETI-search-directions from earlier solver-runs in which case these search-directions are projected out from the overall interface-problem, resulting in the TRKS [9]. This would lead to a reduced solution space and the iterative solver will not have to find the full set of search-directions every time anew. The auxiliary coarse-space adds another constraint

$$\mathbf{C}^T \mathbf{F}^T \vec{r}_k = \vec{0} \quad (4)$$

to the interface-problem with search-space  $\mathbf{C}$  and constraint-space  $\mathbf{FC}$  according to Gaul [8], where  $k$  is the GMRES-iteration counter. Here,  $\mathbf{C}$  contains  $l_2$ -orthonormal search-directions from previous GMRES-solver-runs. This coarse-space  $\mathbf{C}$  is filled up until a predefined coarse-space-size  $N_C$  is reached. To fulfill constraint (4) in each iteration, we construct an auxiliary

coarse-grid projector  $\mathbf{P}_C$ . In the original TRKS for FETI, the projector was described for symmetric systems and a Conjugate Gradient method [9]. In our case, the projector

$$\mathbf{P}_C = \mathbf{I} - \mathbf{F}\mathbf{C}(\mathbf{C}^T\mathbf{F}^T\mathbf{F}\mathbf{C})^{-1}\mathbf{C}^T\mathbf{F}^T \quad \tilde{\mathbf{P}}_C = \mathbf{I} - \mathbf{C}(\mathbf{C}^T\mathbf{F}^T\mathbf{F}\mathbf{C})^{-1}\mathbf{C}^T\mathbf{F}^T\mathbf{F}$$

required some modifications for general matrices  $\mathbf{F}$ , as it is described in [8]. The projector  $\tilde{\mathbf{P}}_C$  is required here for correcting the deflated solution.

This projector is then incorporated into the non-preconditioned GMRES algorithm 1. So, those search-directions, which are stored in  $\mathbf{C}$ , are the first  $N_C$  search-directions generated in the first Newton-Raphson- and GMRES-iterations and reused in all subsequent Newton-Raphson-iterations. From TRKS for the PCPG-algorithm it is known, that search-directions corresponding to high convergence-inhibiting eigenmodes are usually generated in the first iterations, which creates a suitable coarse-space [12]. A similar behavior is expected for the GMRES algorithm.

---

**Algorithm 1:** Two-level GMRES
 

---

```

 $\Delta\vec{\lambda}_0 = \vec{0}, \Delta\hat{\lambda}_0 = \vec{0}$ 
 $\Delta\vec{\lambda}_C = \mathbf{C}(\mathbf{C}^T\mathbf{F}^T\mathbf{F}\mathbf{C})^{-1}\mathbf{C}^T\mathbf{F}^T(\vec{d} - \mathbf{F}\Delta\vec{\lambda}_0)$ 
 $\vec{r}_0 = \vec{d} - \mathbf{F}\Delta\vec{\lambda}_C$ 
 $\vec{w}_0 = \mathbf{P}_C\vec{r}_0$ 
 $\beta = \|\vec{z}_0\|$ 
 $\mathbf{V}_0 = \vec{w}_0/\|\vec{w}_0\|$ 
while  $\|\vec{r}_k\| > \varepsilon_{F,abs}$  and  $\|\vec{r}_k\|/\|\vec{r}_0\| > \varepsilon_{F,rel}$  and  $k \leftarrow 0$  to  $k_{end}$  do
     $\vec{q}_k = \mathbf{F}\mathbf{V}_k$ 
     $\vec{w}_k = \mathbf{P}_C\vec{q}_k$ 
    for  $l \leftarrow 0$  to  $k$  do
         $\mathbf{H}_{l,k} = \vec{w}_k^T\mathbf{V}_l$ 
         $\vec{w}_k = \vec{w}_k - \mathbf{H}_{l,k}\mathbf{V}_l$ 
     $\mathbf{H}_{k+1,k} = \|\vec{w}_k\|, \vec{e}_1 = [0 \ \dots \ 0 \ 1]$ 
     $\vec{u}_k = (\mathbf{H}^T\mathbf{H})^{-1}\mathbf{H}^T(\beta\vec{e}_1)^T$ 
     $\vec{v}_k = \tilde{\mathbf{P}}_C\mathbf{V}\vec{u}_k$ 
     $\vec{r}_k = \vec{r}_0 - \mathbf{F}\vec{v}_k$ 
     $\mathbf{V}_{k+1} = \vec{w}_k/\|\vec{w}_k\|$ 
     $k \leftarrow k + 1$ 
 $\Delta\vec{\lambda} = \Delta\vec{\lambda}_0 + \Delta\vec{\lambda}_C + \vec{v}_k$ 
 $\mathbf{C} = [\mathbf{C} \ \mathbf{V}]$ 

```

---

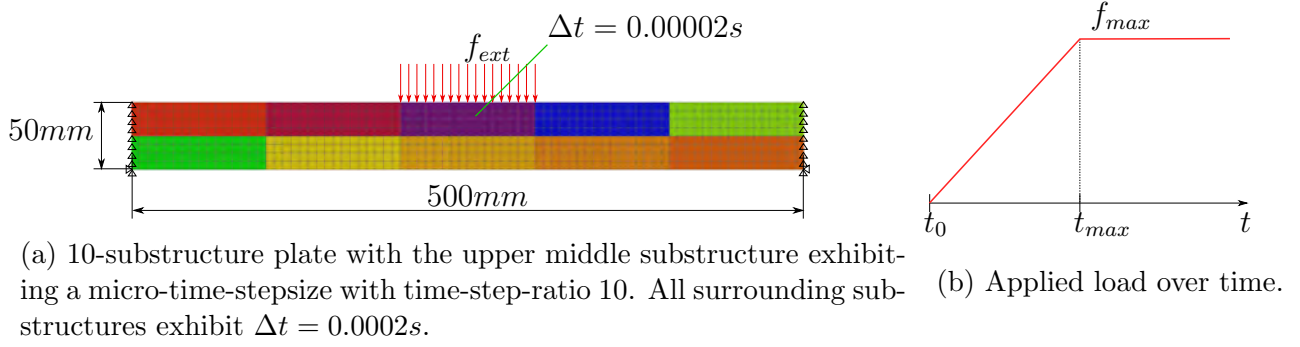


Figure 2: 2D benchmark example with multirate time-integration.

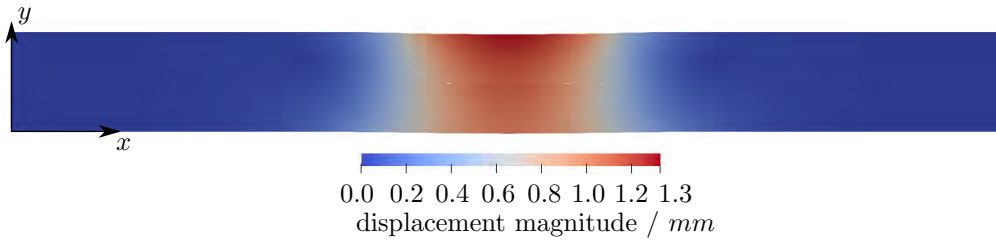


Figure 3: Displacements of converged solution at time 0.001s

### 3 Numerical Experiments

Here, we provide our numerical results. Section 3.1 describes the setup of the presented bending-plate example. In Section 3.2, we investigate the solver's convergence behavior and the captured eigenmodes and in Section 3.3 the influence of the micro-time-scale.

#### 3.1 Model setup

Throughout the following experiments, we used a 2D plate under impact-load as benchmark-example, which is depicted in Fig. 2. This example is composed of 2D rectangular substructures with Quad-4 elements and a geometrically nonlinear St. Venant-Kirchhoff material representing an Aluminium beam (Young's modulus  $E = 70 \cdot 10^3 N/mm^2$ , Poisson's ratio  $\nu = 0.34$ , density  $\rho = 2.7 \cdot 10^{-6} kg/mm^3$ , thickness  $h = 5.0mm$ ). The external load is applied as a ramped up impact-like pressure applied on the middle substructure's top edge, as shown in Fig. 2b with  $f_{max} = 5.0 \cdot 10^3 N/mm$ ,  $t_{max} = 0.001s$ . This model is created in our in-house Open-Source Python-Fortran FE-code AMfe [1] and solved with our Python FETI-library AMfeti [2]. The solvers were set up with absolute tolerances  $\varepsilon_{N,abs} = 1.0 \cdot 10^{-6}$  and  $\varepsilon_{F,abs} = 1.0 \cdot 10^{-7}$  and relative tolerances  $\varepsilon_{N,rel} = 1.0 \cdot 10^{-10}$  and  $\varepsilon_{F,rel} = 1.0 \cdot 10^{-10}$ , such that the Newton-solver is considered converged if either  $max(\|\vec{r}_i^{(s)}\|) < \varepsilon_{N,abs}$  or  $max(\|\vec{r}_i^{(s)}\|)/max(\|\vec{r}_0^{(s)}\|) < \varepsilon_{N,rel}$  and the GMRES is converged if  $\|\vec{r}_k\| < \varepsilon_{F,abs}$  or  $\|\vec{r}_k\|/\|\vec{r}_0\| < \varepsilon_{F,rel}$ . The resulting displacements of the solution at time 0.001s are shown in Figure 3. There are some small incompatibilities visible on the interfaces between the micro- and macro-substructures, resulting from intermediate oscillations in the velocities [18, 15].

#### 3.2 Convergence behavior and capturing eigenmodes

In singlerate dynamics, the PCPG solver's convergence behavior is bounded by the condition-number of the projected preconditioned interface-operator [12, 9]. A GMRES-solver's conver-

rank( $\mathbf{F}$ )	$\mathbf{F}$ size	$\mathbf{F}$ symmetry	$\ \mathbf{F}^T\mathbf{F} - \mathbf{F}\mathbf{F}^T\ $	condition number $\mathbf{A}^{(s)}$	$\mathbf{P}_C\mathbf{F}$ symmetry
240	264 x 264	$1.19 \cdot 10^{-3}$	$4.59 \cdot 10^{-4}$	$2.56 \cdot 10^{19}$	$6.83 \cdot 10^{-2}$
$\ \mathbf{F}^T\mathbf{P}_C^T\mathbf{P}_C\mathbf{F} - \mathbf{P}_C\mathbf{F}\mathbf{F}^T\mathbf{P}_C^T\ $		condition number coarse problem			
$8,51 \cdot 10^{-3}$		$7.33 \cdot 10^2$			

Table 1: System's average characteristic numbers for BGC-macro case with TRKS-projection. Matrix symmetries are checked with  $\|\mathbf{A}^T - \mathbf{A}\|$  for some square matrix  $\mathbf{A}$ .

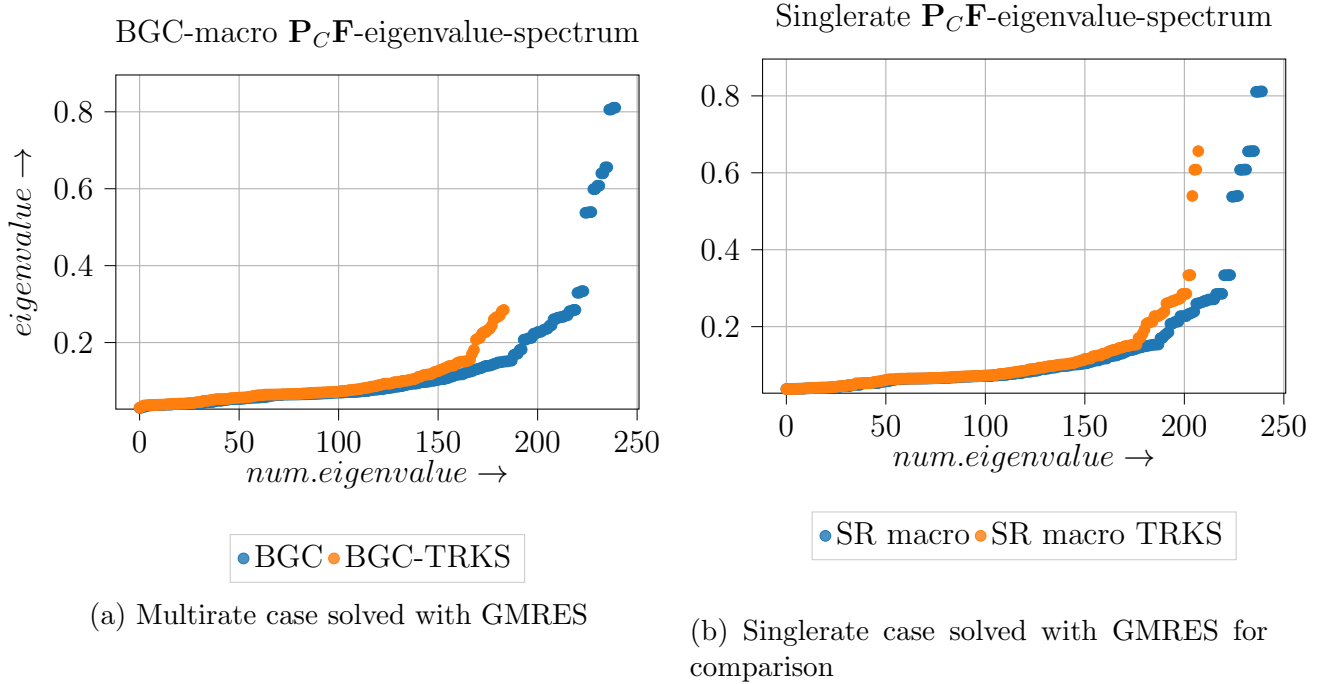
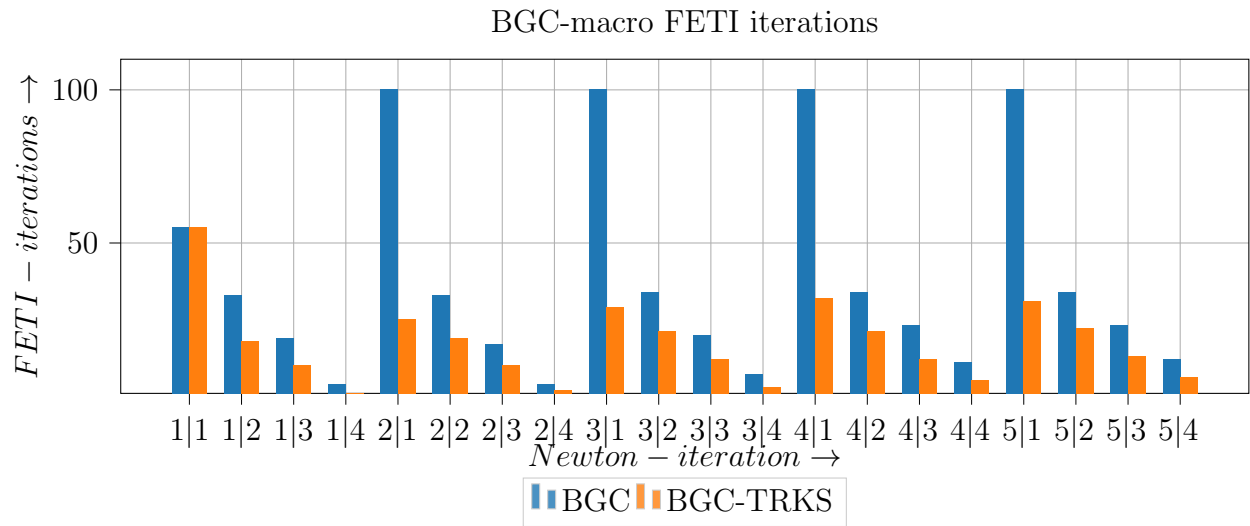
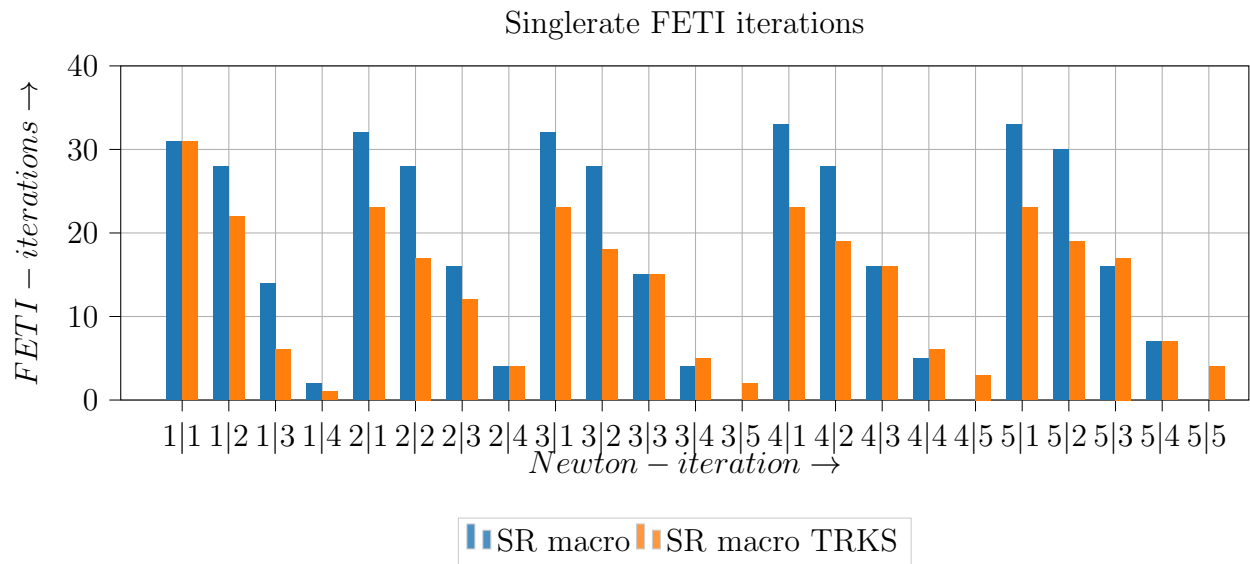


Figure 4: Eigenvalue-spectrum of the eigenvector-matrix of  $\mathbf{P}_C\mathbf{F}$  for multirate and singlerate cases in macro-timestep 1 and Newton-iteration 2.

gence behavior is only determined by this condition-number in case of normal matrices and not necessarily for nonnormal matrices, as pointed out by Greenbaum e.a. [11]. As shown in Table 1, the  $\mathbf{F}$ -operator is indeed a non-normal matrix, which is checked by evaluating  $\|\mathbf{F}^T\mathbf{F} - \mathbf{F}\mathbf{F}^T\|$ : if this norm is close to 0,  $\mathbf{F}$  is considered normal. This also applies for the deflated case with  $\|\mathbf{F}^T\mathbf{P}_C^T\mathbf{P}_C\mathbf{F} - \mathbf{P}_C\mathbf{F}\mathbf{F}^T\mathbf{P}_C^T\|$ . However, one can still formulate an upper bound for the residuals by the condition-number of the eigenvector-matrix of  $\mathbf{P}_C\mathbf{F}$ , as proposed by Gaul [8]. In Figure 4, the eigenvalue-spectra for the BGC-macro case and for the single-rate case (macro-time-step in all substructures) are shown. Note that zero-eigenvalues have been removed in these plots and the eigenvalues are sorted in ascending order. Two aspects arise from these spectra: the eigenspectrum is very similar for both, the BGC-macro and the single-rate case. This implies, that the convergence-behavior is not as much governed by the micro-time-step, but by the macro-time-step. And the other aspect concerns differences in the captured eigenmodes associated to the removed eigenvalues by TRKS. In both cases, the coarse-space-size is limited to 50 and while in the single-rate case some high eigenvalues are kept, they are removed in the BGC-macro case. Krylov solvers capture high eigenmodes first, which lets the TRKS gather these high convergence inhibiting modes early [12]. Hence, a reason for this different behavior might be the initial number of FETI-iterations, as depicted in Figure 5. While in the single-rate case the GMRES-solver requires only 31 iterations in the first timestep and Newton-iteration, 55 are required to solve the interface-problem in the BGC-macro case. This difference with respect



(a) Multirate case solved with GMRES



(b) Singlerate case solved with GMRES for comparison

Figure 5: FETI iterations required to reach convergence for consecutive macro-timesteps and Newton-iterations (see labels  $time-step|Newton-iteration$ ).

to the similar eigenvalue-spectra again emphasizes the fact that the condition number alone does not define the convergence behavior, but it provides a good estimate and describes the behavior of deflation well. That also means that only 31 search-directions are available for the coarse-space and, besides the large eigenvalues, smaller ones are captured in the singlerate-case earlier as well and therefore the coarse-space is enriched with less effective modes. During the subsequent Newton-iterations and time-steps the coarse-space is further filled up. In the BGC-macro case, the coarse-space is completely filled up in the first Newton-iteration. This also improves the relative reduction in the first Newton-iterations compared to the singlerate case. We have to point out, that the GMRES-solver didn't reach convergence in some nondeflated BGC-macro cases, though. However, that is likely a numerical issue related to the bad local conditioning, as the residuals stagnated at a low level, as depicted in Figure 6. Here, deflation

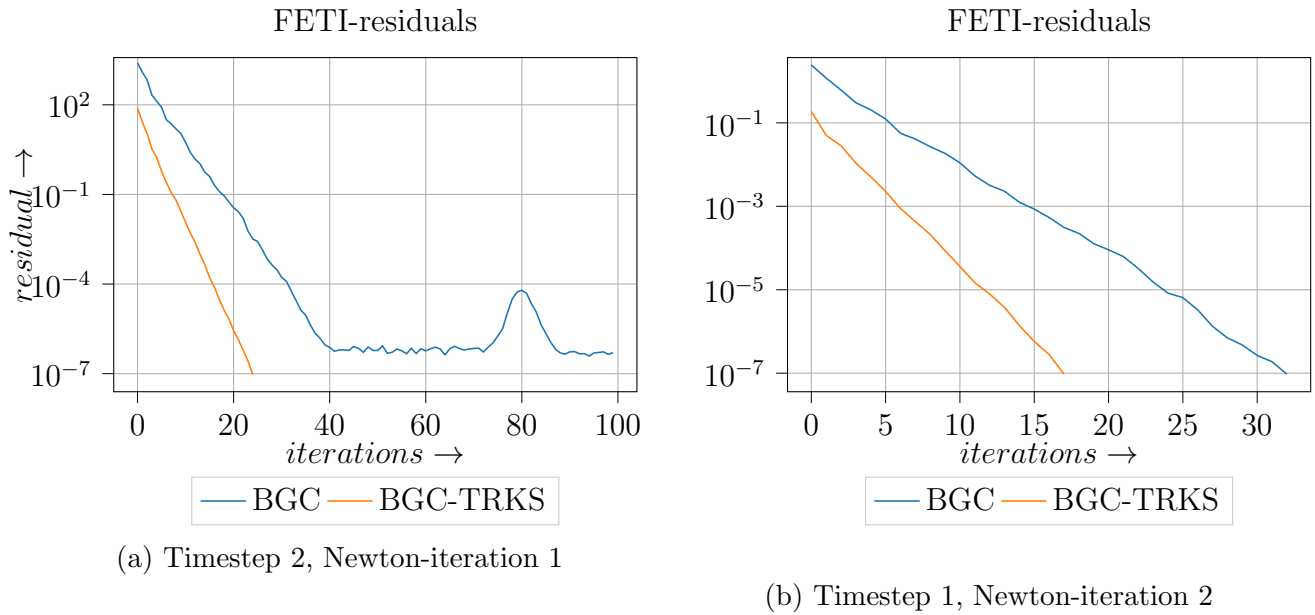
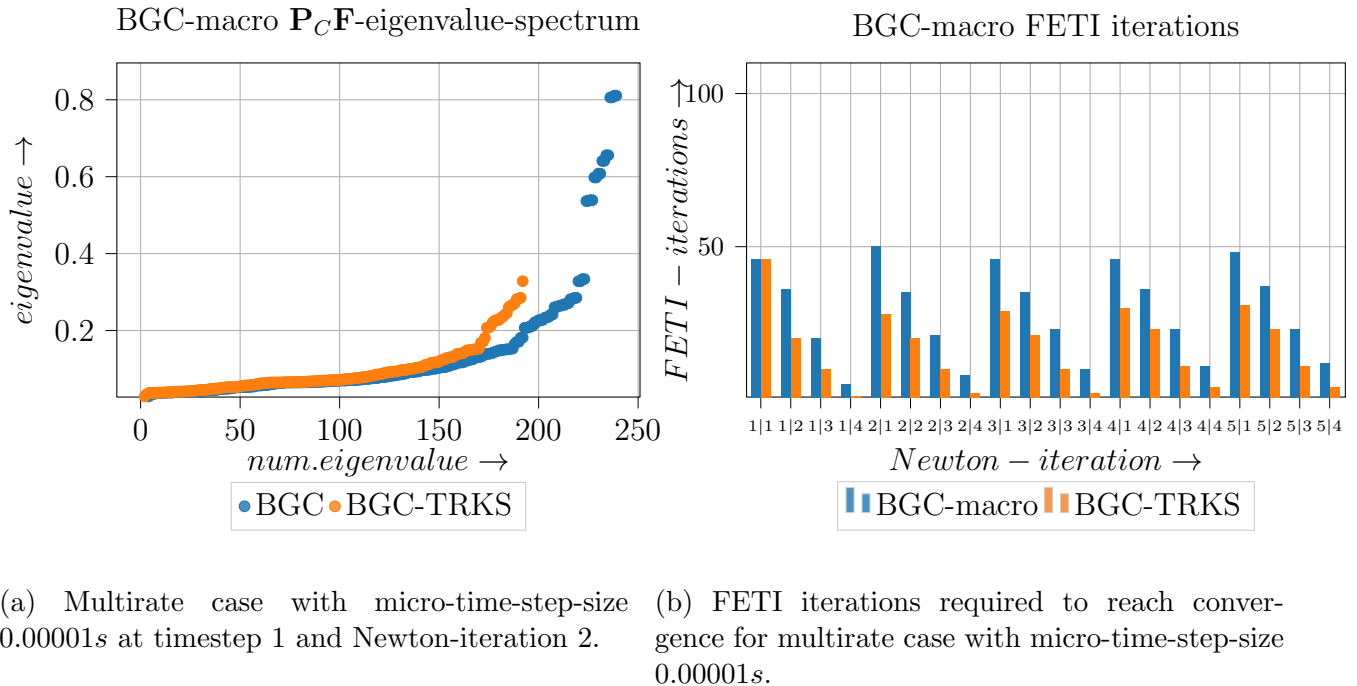


Figure 6: FETI residuals during FETI-iterations of BGC-macro case.



(a) Multirate case with micro-time-step-size 0.00001s at timestep 1 and Newton-iteration 2. (b) FETI iterations required to reach convergence for multirate case with micro-time-step-size 0.00001s.

Figure 7: Eigenvalue-spectrum of the eigenvector-matrix of  $\mathbf{P}_C \mathbf{F}$  and required iterations for multirate case with finer micro-time-scale.

also improved this stability.

### 3.3 Influence of the micro-time-scale

Finally, we further reduce the micro-time-step-size to 0.00001s, resulting in a time-step-ratio of 20. The resulting eigenvalue-spectrum and required FETI-iterations are depicted in Figure 7a and Figure 7b. The eigenvalue spectrum remains very similar to the one with a coarse micro-time-scale in Figure 4a. Hence, the micro-time-scale has limited influence on capturing

the high eigenvalues. The required iterations are slightly reduced, but show similar convergence behavior as in Figure 5a apart from better stability in the nondeflated case.

## 4 CONCLUSIONS

The TRKS has been successfully applied to a GMRES-method for our multirate nonlinear BGC-macro FETI-solver. In our examples, the total recycling approach selects the high convergence inhibiting eigenmodes and therefore improves convergence. Of course, this does not affect the FETI-solver in the first Newton-iteration in the first time-step, as the eigenmodes are to be gathered in this step. With this reducing behavior of the recycling technique and the characteristic deflation of the eigenvalue-spectrum, we can say that recycling is also well applicable to a GMRES-solver and the nonlinear BGC-macro method. Moreover, we found, that the choice of local time-step-sizes hardly affects the performance of the global iterative GMRES-solver. The global Newton- and GMRES-solvers' performances are more governed by the synchronisation- or macro-timestep-size. We are currently working on the application of more selective recycling approaches for multirate methods and the application of preconditioning. Our results in this work also imply, that due to the little interface-problem's dependency of the micro time-steps, reusing search-directions from the singlerate case might be beneficial for a time-adaptive approach and will be investigated further in the future.

**Acknowledgement:** *We thank the DFG for the funding of project RI2451/8-1, in which context this work has been done.*

## REFERENCES

- [1] AMfe, Applied Mechanics Finite Elements Python-Fortran-library, <https://github.com/AppliedMechanics/AMfe>.
- [2] AMfeti, Applied Mechanics Finite Element Tearing and Interconnecting Python-MPI-library, <https://github.com/AppliedMechanics/AMfeti>.
- [3] Brun, M and Gravouil, A. and Combescure, A. and Limam, A. Two FETI-based heterogeneous time step coupling methods for Newmark and  $\alpha$ -schemes derived from the energy method. *Computer Methods in Applied Mechanics and Engineering*, Vol. **283**, pp. 130–176, (2015), doi: 10.1016/j.cma.2014.09.010.
- [4] Farhat, C. and Roux, F.X. A method of finite element tearing and interconnecting and its parallel solution algorithm, *International Journal for Numerical Methods in Engineering*, Vol. **32**, pp. 1205–1227, (1991), doi: 10.1002/nme.1620320604.
- [5] Farhat, C. and Crivelli, L. and Gérardin, M. On the spectral stability of time integration algorithms for a class of constrained dynamics problems, *AIAA/ASME/ASCE/AHS/ASC Structures, Structural Dynamics, and Materials Conference, 34th and AIAA/ASME Adaptive Structures Forum, La Jolla, CA, Apr. 19-22, 1993, Technical Papers. Pt. 1 (A93-33876 13-39)*, pp. 80–97, (1993)
- [6] Farhat, C. and Crivelli, L. and Roux, F.X. A transient FETI methodology for large-scale parallel implicit computations in structural mechanics, *International Journal for Numerical Methods in Engineering*, Vol. **37**, pp. 1945–1975, (1994), doi: 10.1002/nme.1620371111.
- [7] Farhat, C. and Kendall, P. and Lesoinne, M. The second generation FETI methods and their application to the parallel solution of large-scale linear and geometrically non-linear

- structural analysis problems. *Computer methods in applied mechanics and engineering*, Vol. **184**, pp. 333–374, (2000), doi: 10.1016/S0045-7825(99)00234-0
- [8] Gaul, A. Recycling Krylov subspace methods for sequences of linear systems - Analysis and applications. *Technische Universität Berlin*, Dissertation, (2014), [https://depositonce.tu-berlin.de/bitstream/11303/4444/1/gaul\\_andre.pdf](https://depositonce.tu-berlin.de/bitstream/11303/4444/1/gaul_andre.pdf).
- [9] Gosselet, P. and Rey, C. and Pebrel, J. Total and selective reuse of Krylov subspaces for the resolution of sequences of nonlinear structural problems, *International Journal for Numerical Methods in Engineering*, Vol. **94**, pp. 60–83, (2013), doi: 10.1002/nme.4441.
- [10] Gravouil, A. and Combescure, A. Multi-time-step explicit - Implicit method for nonlinear structural dynamics, *International Journal for Numerical Methods in Engineering*, Vol. **50**, pp. 199–225, (2001), doi: 10.1002/1097-0207(20010110)50:1<199::AID-NME132>3.0.CO;2-A.
- [11] Greenbaum, A. and Pták, V. and Strakoš, Z. Any Nonincreasing Convergence Curve is Possible for GMRES, *Society for Industrial and Applied Mathematics*, Vol. **17**, pp. 465–469, (1996)
- [12] Leistner, M. C. and Gosselet, P. and Rixen, D. J. Recycling of solution spaces in multi-preconditioned FETI methods applied to structural dynamics, *International Journal for Numerical Methods in Engineering*, Vol. **116**, pp. 141–160, (2018), doi: 10.1002/nme.5918.
- [13] Leyendecker, S. and Ober-Blöbaum, S. A variational approach to multirate integration for constrained systems, *Multibody Dynamics 2011, ECCOMAS Thematic Conference, Brussels, Belgium, 4-7 July 2011*, pp. 1–15, (2011).
- [14] Newmark, N.M. Method of Computation for Structural Dynamics, *Journal of the Engineering Mechanics Division*, Vol. **85**, pp. 67–94, (1959).
- [15] Prakash, A. and Taciroglu, E. and Hjelmstad, K. D. Computationally efficient multi-time-step method for partitioned time integration of highly nonlinear structural dynamics. *Computers and Structures*, Vol. **133**, pp. 51–63, (2014), doi: 10.1016/j.compstruc.2013.11.013.
- [16] Saad, Y. and Schultz, M. H. GMRES: A Generalized Minimal Residual Algorithm for Solving Nonsymmetric Linear Systems. *SIAM Journal on Scientific and Statistical Computing*, Vol. **7**, pp. 856–869, (1986), doi: 10.1137/0907058
- [17] Seibold, A. S. and Leistner, M. C. and Rixen, D. J. Localization of nonlinearities and recycling in dual domain decomposition. *Domain Decomposition Methods in Science and Engineering XXV*, pp. 474–482, (2018), doi: 10.1007/978-3-030-56750-7, isbn: 978-3-030-56749-1.
- [18] Seibold, A. S. and Rixen, D. J. A variational approach to asynchronous time-integration of structural dynamics problems in the context of FETI and spurious oscillations on the interfaces. *EURODYN 2020, XI International Conference on Structural Dynamics*, pp. 26–43, (2020), doi: 10.47964/1120.9003.19111.
- [19] Seibold, A. S. and Rixen, D. J. Preconditioning of a FETI-solver for a nonlinear asynchronous time-integrator applied to structural dynamics. *PAMM*, pp. 1–2, (2021), doi: 10.1002/pamm.202000213.

- [20] Yeung, M.C. and Tang, J.M. and Vuik, C. On the Convergence of GMRES with Invariant-Subspace Deflation. *Reports of the Delft Institute of Applied Mathematics*, pp. 1–35, (2010), issn: 1389-6520.